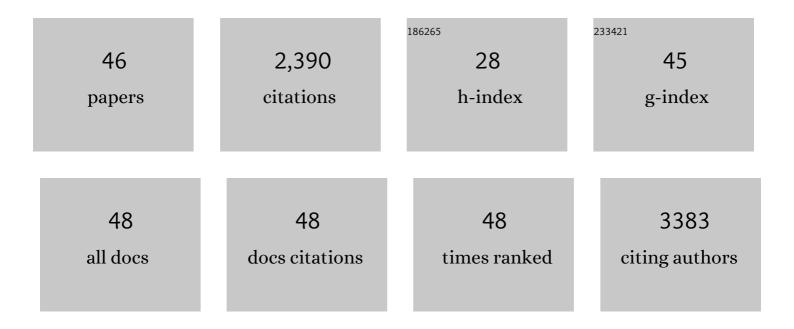
Thorsten Mielke

List of Publications by Year in descending order

Source: https://exaly.com/author-pdf/2048025/publications.pdf Version: 2024-02-01



#	Article	IF	CITATIONS
1	Structure of the mammalian ribosome as it decodes the selenocysteine UGA codon. Science, 2022, 376, 1338-1343.	12.6	27
2	Steps toward translocation-independent RNA polymerase inactivation by terminator ATPase Ï• Science, 2021, 371, .	12.6	78
3	Protein Synthesis in the Developing Neocortex at Near-Atomic Resolution Reveals Ebp1-Mediated Neuronal Proteostasis at the 60S Tunnel Exit. Molecular Cell, 2021, 81, 304-322.e16.	9.7	27
4	Unc13A and Unc13B contribute to the decoding of distinct sensory information in Drosophila. Nature Communications, 2021, 12, 1932.	12.8	16
5	Snapshots of native pre-50S ribosomes reveal a biogenesis factor network and evolutionary specialization. Molecular Cell, 2021, 81, 1200-1215.e9.	9.7	35
6	Putative Cooperative ATP–DnaA Binding to Double-Stranded DnaA Box and Single-Stranded DnaA-Trio Motif upon Helicobacter pylori Replication Initiation Complex Assembly. International Journal of Molecular Sciences, 2021, 22, 6643.	4.1	9
7	Dnmt1 has de novo activity targeted to transposable elements. Nature Structural and Molecular Biology, 2021, 28, 594-603.	8.2	83
8	Temporal compartmentalization of viral infection in bacterial cells. Proceedings of the National Academy of Sciences of the United States of America, 2021, 118, .	7.1	7
9	Structural insights into Cullin4-RING ubiquitin ligase remodelling by Vpr from simian immunodeficiency viruses. PLoS Pathogens, 2021, 17, e1009775.	4.7	11
10	Structures of active melanocortin-4 receptor–Gs-protein complexes with NDP-α-MSH and setmelanotide. Cell Research, 2021, 31, 1176-1189.	12.0	40
11	The role of <i>Helicobacter pylori</i> DnaA domain I in orisome assembly on a bipartite origin of chromosome replication. Molecular Microbiology, 2020, 113, 338-355.	2.5	5
12	Structure-Based Mechanisms of a Molecular RNA Polymerase/Chaperone Machine Required for Ribosome Biosynthesis. Molecular Cell, 2020, 79, 1024-1036.e5.	9.7	41
13	Estrogens Determine Adherens Junction Organization and E-Cadherin Clustering in Breast Cancer Cells via Amphiregulin. IScience, 2020, 23, 101683.	4.1	14
14	Endocytosis-Mediated Replenishment of Amino Acids Favors Cancer Cell Proliferation and Survival in Chromophobe Renal Cell Carcinoma. Cancer Research, 2020, 80, 5491-5501.	0.9	11
15	The microfollicle: a model of the human hair follicle for in vitro studies. In Vitro Cellular and Developmental Biology - Animal, 2020, 56, 847-858.	1.5	12
16	Cryo-EM structure of the Shigella type III needle complex. PLoS Pathogens, 2020, 16, e1008263.	4.7	36
17	Cryo-EM structures reveal intricate Fe-S cluster arrangement and charging in Rhodobacter capsulatus formate dehydrogenase. Nature Communications, 2020, 11, 1912.	12.8	48
18	Cell type-dependent differential activation of ERK by oncogenic KRAS in colon cancer and intestinal epithelium. Nature Communications, 2019, 10, 2919.	12.8	70

THORSTEN MIELKE

#	Article	IF	CITATIONS
19	Structural transitions during the scaffolding-driven assembly of a viral capsid. Nature Communications, 2019, 10, 4840.	12.8	21
20	Structural Basis for the Action of an All-Purpose Transcription Anti-termination Factor. Molecular Cell, 2019, 74, 143-157.e5.	9.7	86
21	Mechanistic insights into the role of prenyl-binding protein PrBP/δ in membrane dissociation of phosphodiesterase 6. Nature Communications, 2018, 9, 90.	12.8	13
22	Simple paired heavy- and light-chain antibody repertoire sequencing using endoplasmic reticulum microsomes. Genome Medicine, 2018, 10, 34.	8.2	13
23	It takes two transducins to activate the cCMP-phosphodiesterase 6 in retinal rods. Open Biology, 2018, 8, .	3.6	34
24	tRNA Translocation by the Eukaryotic 80S Ribosome and the Impact of GTP Hydrolysis. Cell Reports, 2018, 25, 2676-2688.e7.	6.4	61
25	Structure and Function of the Campylobacter jejuni Chromosome Replication Origin. Frontiers in Microbiology, 2018, 9, 1533.	3.5	11
26	Structural Visualization of the Formation and Activation of the 50S Ribosomal Subunit during InÂVitro Reconstitution. Molecular Cell, 2018, 70, 881-893.e3.	9.7	46
27	Human iPSC-Derived Neural Progenitors Are an Effective Drug Discovery Model for Neurological mtDNA Disorders. Cell Stem Cell, 2017, 20, 659-674.e9.	11.1	126
28	Structural basis for λN-dependent processive transcription antitermination. Nature Microbiology, 2017, 2, 17062.	13.3	58
29	De Novo Mutations in SLC25A24 Cause a Craniosynostosis Syndrome with Hypertrichosis, Progeroid Appearance, and Mitochondrial Dysfunction. American Journal of Human Genetics, 2017, 101, 833-843.	6.2	56
30	Stable Positioning of Unc13 Restricts Synaptic Vesicle Fusion to Defined Release Sites to Promote Synchronous Neurotransmission. Neuron, 2017, 95, 1350-1364.e12.	8.1	106
31	Footprint-free human fetal foreskin derived iPSCs: A tool for modeling hepatogenesis associated gene regulatory networks. Scientific Reports, 2017, 7, 6294.	3.3	9
32	Spermidine Suppresses Age-Associated Memory Impairment by Preventing Adverse Increase of Presynaptic Active Zone Size and Release. PLoS Biology, 2016, 14, e1002563.	5.6	82
33	Structural insights into ribosomal rescue by Dom34 and Hbs1 at near-atomic resolution. Nature Communications, 2016, 7, 13521.	12.8	42
34	Structures of ribosome-bound initiation factor 2 reveal the mechanism of subunit association. Science Advances, 2016, 2, e1501502.	10.3	59
35	Quantitative interaction mapping reveals an extended UBX domain in ASPL that disrupts functional p97 hexamers. Nature Communications, 2016, 7, 13047.	12.8	35
36	Molecular architecture of the ribosomeâ€bound Hepatitis C Virus internal ribosomal entry site <scp>RNA</scp> . EMBO Journal, 2015, 34, 3042-3058.	7.8	80

THORSTEN MIELKE

#	Article	IF	CITATIONS
37	Parallel Structural Evolution of Mitochondrial Ribosomes and OXPHOS Complexes. Genome Biology and Evolution, 2015, 7, 1235-1251.	2.5	77
38	Cryo-EM of Ribosomal 80S Complexes with Termination Factors Reveals the Translocated Cricket Paralysis Virus IRES. Molecular Cell, 2015, 57, 422-432.	9.7	82
39	Structural Snapshots of Actively Translating Human Ribosomes. Cell, 2015, 161, 845-857.	28.9	161
40	Architecture of Polyglutamine-containing Fibrils from Time-resolved Fluorescence Decay. Journal of Biological Chemistry, 2014, 289, 26817-26828.	3.4	9
41	Cryo-electron Microscopic Structure of SecA Protein Bound to the 70S Ribosome. Journal of Biological Chemistry, 2014, 289, 7190-7199.	3.4	35
42	Structure of the mammalian 80S initiation complex with initiation factor 5B on HCV-IRES RNA. Nature Structural and Molecular Biology, 2014, 21, 721-727.	8.2	97
43	Regulation of the Mammalian Elongation Cycle by Subunit Rolling: A Eukaryotic-Specific Ribosome Rearrangement. Cell, 2014, 158, 121-131.	28.9	125
44	Assembly of Helicobacter pylori Initiation Complex Is Determined by Sequence-Specific and Topology-Sensitive DnaA–oriC Interactions. Journal of Molecular Biology, 2014, 426, 2769-2782.	4.2	33
45	Structure of the no-go mRNA decay complex Dom34–Hbs1 bound to a stalled 80S ribosome. Nature Structural and Molecular Biology, 2011, 18, 715-720.	8.2	150
46	Mechanism of elF6-mediated Inhibition of Ribosomal Subunit Joining. Journal of Biological Chemistry, 2010, 285, 14848-14851.	3.4	107